

Numerical Modelling and Field Measurements for Wave Resource Characterization

Zhaoqing Yang^{#1}, Wei-Cheng Wu^{#2}, Taiping Wang^{#3}, Gabriel García-Medina^{#4}, Levi Kilcher^{*5}

[#]*Pacific Northwest National Laboratory*

1100 Dexter Ave N, Ste 500, Seattle, WA 98006 USA

¹zhaoqing.yang@pnnl.gov

²wei-cheng.wu@pnnl.gov

³taiping.wang@pnnl.gov

⁴gabriel.garciamedina@pnnl.gov

^{*}*National Renewable Energy Laboratory*

15013 Denver West Parkway, Golden, CO 80401, USA

⁵levi.kilcher@nrel.gov

Abstract — Wave resource characterization is an essential step for Wave Energy Converter (WEC) development. The West Coast is one of the top regions in the U.S. with an energetic wave energy resource and great potential for early market development. This paper presents a study using a multi-scale modelling approach combined with shallow water wave measurements to improve the accuracy of wave resource characterization. The multi-scale wave modelling was conducted with a nested-grid WaveWatchIII (WW3) model from global to regional scales. The Unstructured-grid Simulating Waves Nearshore (UnSWAN) model was used to provide accurate wave hindcast with a resolution of approximately 300 m, which meets the requirement recommended by IEC for wave resource assessment and characterization for the feasibility class. Extensive model validation for a period of 32 years was conducted using measured data from wave buoys maintained by National Data Buoy Center, as well as from three recently deployed nearshore buoys along the Oregon and California coasts. Inter-annual and seasonal variations of wave characteristics along the entire West Coast was analyzed. In addition, a sensitivity analysis was carried out to evaluate the quality of wind forcing on the accuracy of model prediction for large waves.

Keywords — Wave Energy, Resource Characterization, Modelling, Measurements, Multi-scale and -resolution

I. INTRODUCTION

The U.S. West Coast has the second largest wave resource among all U.S. major coastal regions, as reported in a nationwide wave resource assessment study [1], which was based on the 4-arc minute spatial resolution wave hindcasts generated by the National Oceanic and Atmospheric Administration (NOAA) using the WaveWatchIII (WW3) model [2]. The nearshore regions have the most promising market for wave energy converter (WEC) development because of low costs for deployment and maintenance, as well as low operational risk under extreme events [3]. However, 4-arc minute spatial resolution of WW3 hindcast may not be sufficient to quantify the resource accurately in the nearshore regions. Therefore, there is a need to increase the model resolution in the nearshore

areas [4], especially for feasibility class assessment as recommended by the International Electrotechnical Commission (IEC) Technical Specification for wave resource assessment [5].

It is challenging to simulate wave climates at a regional scale with a fine grid resolution because of the need of high computational resource. There have been a number of studies on wave climate in the U.S. Pacific Northwest coast using a nested-grid modelling approach with structured-grid WW3 and SWAN models [6-8]. Unstructured-grid wave models provide the advantage of combining grid resolution flexibility with computational efficiency for a large model domain [9-14].

In this study, a modelling approach with nested-grid WW3 from global to regional scales and high-resolution unstructured-grid SWAN (UnSWAN) [12] was applied to simulate high resolution wave climates along the U.S. West Coast. Model results for simulating the IEC wave resource parameters were validated with wave measurements within the model domain. Model skills, wave climates and seasonal variability in the nearshore region of the west coast were analyzed based on a 32-year wave hindcast produced by the high-resolution UnSWAN model.

II. METHODS

In this study, a modelling approach with multi-scale, multi-resolution numerical models, combined with high quality wave measurements was performed to improve wave resource characterization in the nearshore region of the U.S. West Coast.

A. Numerical Modelling

The numerical modelling component consists of nested WW3 models at global to regional scales and a high-resolution unstructured-grid SWAN model for the nearshore region along the entire west coast. Three levels of nested grids with WW3 were set up to simulate wave climates from global to regional scales and provide open boundary conditions to the high-resolution UnSWAN model for the west coast. The level 3

WW3 grid with 1-arc minute resolution as well as the UnSWAN model domains are shown in *Fig. 1*. ST4 physics package in WW3 was used in WW3 simulations, based on the sensitivity analysis on a wave model test bed study.

The unstructured-grid UnSWAN model covers the coast from the south end of Vancouver Island, Canada, to southern California. The open boundary of the UnSWAN model domain was specified approximately 25 to 30 km offshore, with a grid resolution of around 300 m in the nearshore shallow-water region. Model bathymetries for both WW3 and UnSWAN models were interpolated from the NOAA 3 arc second (90 m) Coastal Relief Model for the inner shelf region and the NOAA 1 arc minute ETOPO1 Global Relief Model for the outer shelf and deep basin.

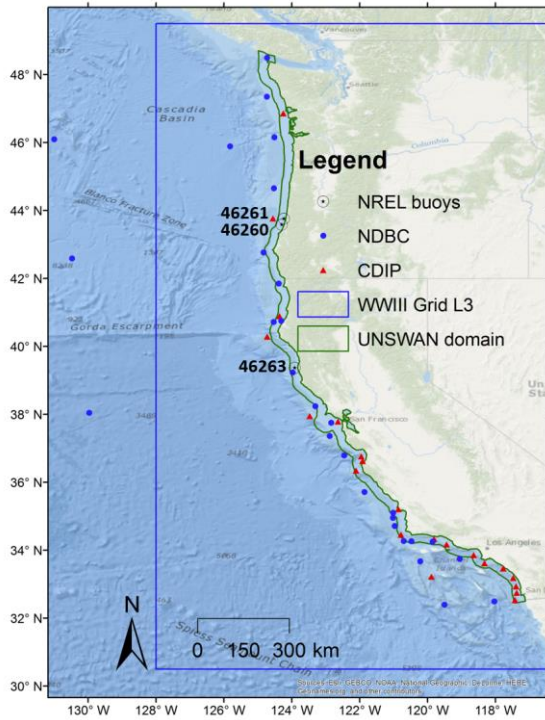


Fig. 1 Model domains of US West Coast and buoy locations for model validation. Blue line represents the Level 3 WW3 model domain and green line represents the nearshore high resolution UnSWAN model domain. Buoy 46260, 46261 and 46263 were deployed by NREL and maintained by CDIP.

Wind forcing to drive the WW3 and UnSWAN models were obtained from the Climate Forecast System Reanalysis (CFSR), simulated by the NOAA National Centers for Environmental Prediction (NCEP) at 0.5° spatial resolution and hourly intervals. The model configurations are consistent with the test bed study by Yang et al. [8]. Both WW3 and UnSWAN models used 24 direction bins with a uniform resolution of 15 degrees and 29 frequency bins with a minimum frequency of 0.035 Hz and a maximum frequency of 0.505 Hz. Detailed model configurations of WW3 and UnSWAN, including model grid resolutions, run-time steps and selected source terms are provided in Yang et al. [15].

B. Field Measurements

While there are many wave measurement data available for model validation at NDBC and CDIP buoys (*Fig. 1*), high quality data in the nearshore shallow water region is limited. To support model validation, especially in the nearshore region, three directional waverider buoys were deployed in the nearshore region off Oregon and northern California coasts.

The waverider buoys were deployed at depths of 87 m (46260, Lakeside, OR), 44 m (46261, Reedsport, OR), and 130 m (46263, Fort Bragg, CA), thus measuring waves in intermediate to shallow waters. These types of buoys are capable of accurately measuring waves with periods from 1.6 to 30 s, which include long period swells from distant sources that reach the U.S. West Coast.



Fig. 2 Waverider buoys deployed in Lakeside, OR (#46260, left) and Fort Bragg, CA (#46263, right).

III. RESULTS

A 32-year wave hindcast, from January 1, 1979 to December 31, 2010, was conducted using a nested-grid modelling approach with WW3 and UnSWAN. Directional spectral model outputs from WW3 were used to drive the nearshore high-resolution UnSWAN model for the west coast. Examples of global distributions of CFSR wind speed and significant wave height simulated with the nested-grid WW3 for January are shown in *Fig. 3* and *Fig. 4*, respectively.

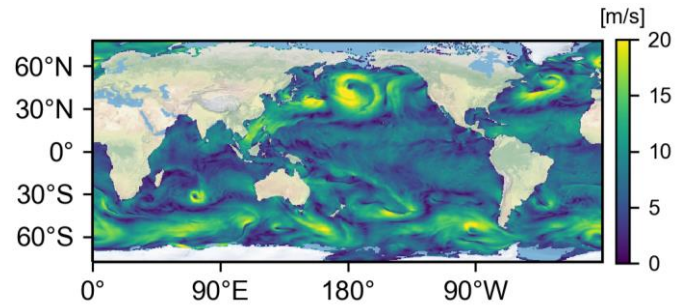


Fig. 3 Global CFSR wind speed distribution on January 13, 2009. Wind over land is not shown.

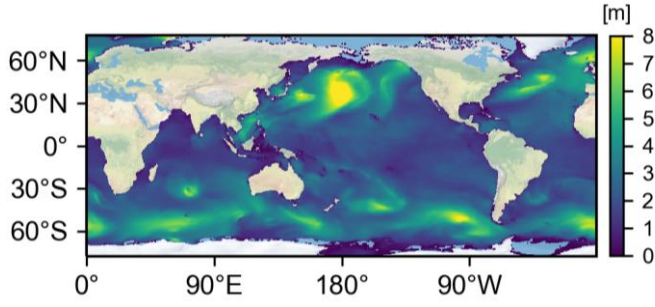


Fig. 4 Simulated global significant wave height on January 13, 2009 with nested grid WW3.

A. Model Validation

Extensive model validation was conducted using observed data from buoys maintained by National Data Buoy Center (NDBC) and the Coastal Data Information Program (CDIP). Specifically, the six simulated IEC wave resource parameters were compared to those derived from observed data at 28 wave buoys. The model skill statistics, including root-mean-square-error (RMSE), linear correlation coefficient (R), percentage error, scatter index and bias were calculated for omnidirectional wave power J_{omni} , significant wave height H_{m0} , energy period T_e , spectral width ϵ_0 , direction of maximum directionally resolved wave power θ , and the directionality coefficient d_θ [15]. The spatial and temporal averaged RMSE and R for the six simulated IEC wave resource parameters for WA, OR and CA coasts are provided in Table 1. Overall, the modeling skills in simulating the six IEC parameters in the west coast are in very good agreement with measurements.

Table 1 Averaged error statistics (RMSE and R) of the six simulated IEC wave resource parameters along WA, OR and CA coasts

Parameter	RMSE			R		
	WA	OR	CA	WA	OR	CA
J (kW/m)	18.78	18.38	10.64	0.91	0.93	0.87
H_s (m)	0.39	0.38	0.33	0.94	0.95	0.88
T_e (s)	1.19	1.28	1.29	0.88	0.89	0.84
ϵ_0 (-)	0.07	0.07	0.07	0.67	0.67	0.67
θ (degrees)	18	25	20	0.68	0.72	0.65
d_θ (-)	0.27	0.17	0.12	0.45	0.42	0.46

Time series comparison of significant wave height at the three newly deployed buoy stations are shown in Fig. 5, for the period of January 1 to April 1, 2018. The model generally performed very well in capturing the dynamic variability of wave climates at the intermediate to shallow water depths. Fig. 5 also indicated that wave energy in the Oregon Coast (buoy 46260 and 46261) is much larger than the wave energy in California Coast (buoy 46263).

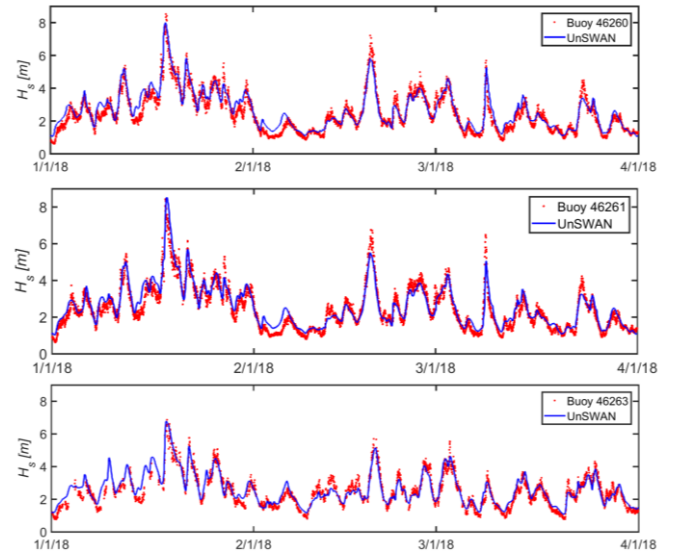


Fig. 5 Comparison of simulated and observed significant wave height at buoy 46260 (upper panel), 46261 (middle panel) and 46263 (lower panel).

To further evaluate the performance of high-resolution UnSWAN, simulated monthly averaged significant wave heights along the 50 m isobath in the west coast were compared to those simulated with NCEP 4' resolution WW3. Fig. 6 shows that the 4' resolution WW3 tends to under-predict the significant wave height compared to UnSWAN results, for both winter (December) and Summer (August) seasons. Therefore, there coarse grid WW3 may underestimate the resource in the shallow-water regions.

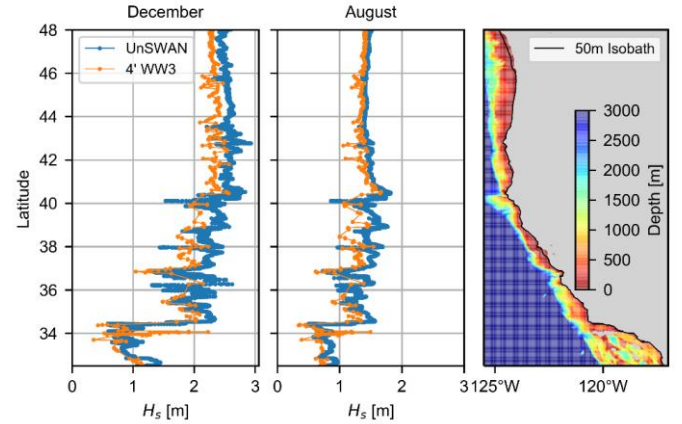


Fig. 6 Comparison of simulated monthly-average significant wave heights with WW3 UnSWAN for the west coast in December (left) and August (middle). The model bathymetry and 50m isobath are shown in the right panel.

B. Sea-States Analysis

Characterization of sea-states is important for WEC design and optimal siting. Fig. 7 shows the horizontal 2D distributions of simulated monthly significant wave heights and wave peak period with UnSWAN in December and August. Clearly, significant wave height in the west coast in December (winter) is much greater than that in August. Fig. 7

(a, b) also indicates that wave resource in WA, OR and Northern CA coasts are much higher and have greater seasonality than that in the southern CA coast. It is interesting to see that while wave peak period has strong seasonal variability similar to significant wave height, wave period in the southern CA coast not only shows little seasonal variability but also longer wave period than the rest of the regions.

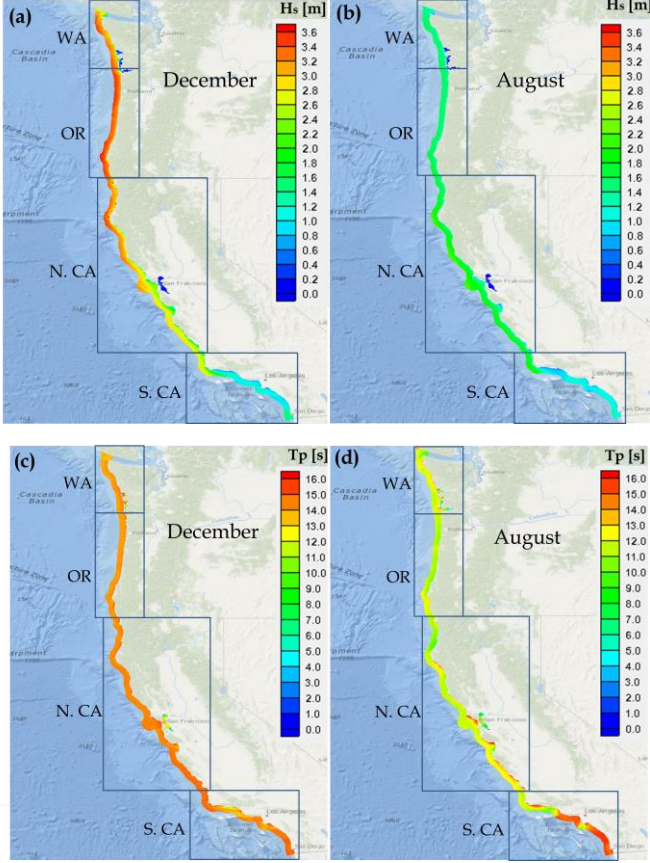


Fig. 7 Simulated monthly-average significant wave height for (a) December and (b) August, and peak period for (c) December and (d) August.

Six sea-state conditions were analyzed, including unimodal wind-sea and swell as well as four multimodal conditions. The sea-state analysis was conducted based on hourly spectral partition output from the high-resolution UnSWAN hindcast for the 32-year period, from 1979 to 2010. The occurrence of each sea-state was calculated as the percentage of the number of time steps for which wave climate is observed over the total number of time steps in the partition output

$$Occ(\%) = \frac{N_{\text{wave climate}}}{N_{\text{total}}} \cdot 100\%$$

Monthly-averaged sea-states based on 32-year model partition outputs were quantified for each sub-regions, i.e., WA, OR, N. CA and S. CA coasts. Final results of sea-state conditions for December and August are summarized in Table 2. The unimodal wind-sea condition occurs less than 4% of

the time regardless of the region, suggesting the dominance of swells in the west coast. The monthly-average occurrence of the unimodal swell conditions increases by 15% to 25% from summer to winter for all regions except S. CA. There is a clear trend that swells become more and more dominant from the southern coast to the northern coast. However, in August, sea-states for the entire west coast are primarily dominated by multi-modal conditions, especially four- and higher-modals.

Table 2 Occurrence of wave climates for December (blue) and August (red)

Wave Climates	S. CA	N. CA	OR	WA
Unimodal				
Wind-Sea	0.03	0.5	4.0	3.4
	0.01	0.02	0.03	0.03
Swell	4.9	15.6	25.3	24.8
	0.01	0.02	0.03	0.03
Multimodal				
Wind-Sea + 1 Swell	0.4	1.8	6.5	6.3
	0.8	1.7	1.9	1.4
2 Swells	17.0	26.4	26.3	27.4
	4.5	5.9	12.1	15.8
Wind-Sea + 2 Swells	6.7	5.8	8.2	9.7
	20.4	25.6	20.0	11.9
All others	70.9	49.8	29.8	28.4
	74.1	66.7	65.7	69.1

IV. CONCLUSIONS

In this study, the unstructured-grid wave model, UnSWAN, was applied to simulate wave fields in the U.S. West Coast, with open boundary conditions provided by nested-grid global and regional WW3 model. Model performance for simulating the six IEC resource parameters was evaluated with buoy observations, especially with shallow-water buoy data. Model results showed higher seasonal variability in significant wave height and wave peak period on the WA, OR, and N. CA coasts than the S. CA coast.

In general, wind-sea condition is very small along the entire west coast, throughout the year. Unimodal and bimodal swells are dominant in WA and OR coasts in December. In summer, the sea-state of all regions is dominated by the presence of higher-modal conditions. However, in winter, this dominance is largely reduced in WA and OR coasts. This study also indicated that the high-resolution UnSWAN improved wave resource hindcast compared to the results from the 4' resolution WW3 model. The effect of complicated bathymetric features such as canyons and headlands are well represented in the UnSWAN model because of the advantage of high resolution and flexible mesh.

ACKNOWLEDGMENT

This study was funded by the Water Power Technologies Office under the Office of Energy Efficiency and Renewable Energy, U.S. Department of Energy.

REFERENCES

1. EPRI, *Mapping and Assessment of the United States Ocean Wave Energy Resource*, in *EPRI 2011 Technical Report to U.S. Department of Energy* 2011, Electric Power Research Institute: Palo Alto, California.
2. Tolman, H.L. and WAVEWATCH III Development Group, *User manual and system documentation of WAVEWATCH III® version 4.18*, 2014, National Oceanic and Atmospheric Administration, National Weather Service, National Centers for Environmental Prediction: College Park, MD 20740. p. 311.
3. Drew, B., A.R. Plummer, and M.N. Sahinkaya, *A review of wave energy converter technology*. Proceedings of the Institution of Mechanical Engineers Part a-Journal of Power and Energy, 2009. **223**(A8): p. 887-902.
4. Morim, J., N. Cartwright, A. Etemad-Shahidi, D. Strauss, and M. Hemer, *Wave energy resource assessment along the Southeast coast of Australia on the basis of a 31-year hindcast*. Applied Energy, 2016. **184**: p. 276-297.
5. IEC, *Marine energy – wave, tidal and other water current converters – Part 101: Wave energy resource assessment and characterization*, 2015, International Electrotechnical Commission: Geneva, Switzerland.
6. García-Medina, G., H.T. Özkan-Haller, P. Ruggiero, and J. Oskamp, *An Inner-Shelf Wave Forecasting System for the U.S. Pacific Northwest*. Weather and Forecasting, 2013. **28**(3): p. 681-703.
7. García-Medina, G., H.T. Özkan-Haller, and P. Ruggiero, *Wave resource assessment in Oregon and southwest Washington, USA*. Renewable Energy, 2014. **64**: p. 203-214.
8. Yang, Z., V.S. Neary, T. Wang, B. Gunawan, A.R. Dallman, and W. Wu, *A wave model test bed study for wave energy resource characterization*. Renewable Energy, 2017.
9. Roland, A., *Development of WWM II: Spectral wave modelling on unstructured meshes.*, in *Institute of Hydraulic and Water Resources Engineering*. 2009, Technische Universität Darmstadt.
10. Zijlema, M., *Computation of wind-wave spectra in coastal waters with SWAN on unstructured grids*. Coastal Engineering, 2010. **57**(3): p. 267-277.
11. Gagnaire-Renou, E., M. Benoit, and P. Forget, *Spectral wave modeling using a quasi-exact method for nonlinear wave-wave interactions*. Houille Blanche-Revue Internationale De L Eau, 2012(3): p. 51-60.
12. SWAN, *SWAN: User Manual, Cycle III version 41.01A*, 2015, Delft University of Technology: Delft, The Netherlands.
13. Roland, A., Y.J. Zhang, H.V. Wang, Y.Q. Meng, Y.C. Teng, V. Maderich, I. Brovchenko, M. Dutour-Sikiric, and U. Zanke, *A fully coupled 3D wave-current interaction model on unstructured grids*. Journal of Geophysical Research-Oceans, 2012. **117**.
14. Wu, W.-C., Z. Yang, and T. Wang, *Wave Resource Characterization Using an Unstructured Grid Modeling Approach*. Energies, 2018. **11**(3): p. 15.
15. Yang, Z., W.C. Wu, T. Wang, and L. Castrucci, *Regional Wave Hindcast for the U.S. West Coast*, 2018, PNNL: Richland, WA.